

Geochemistry and Tectonic Setting of the Metagabbros of Penjween Ophiolite Complex, Northeastern Iraq

Omar S. Al-Taweel¹, Flyah H. Al-Khatony²,
Mohammed A. Al-Jboury³, Shareef Th. Al-Hamed⁴

^{1,2,3,4}Department of Geology, College of Science, University of Mosul, Mosul, Iraq

Received 12th June 2022; Accepted 26th October 2022

Abstract

The Penjween Ophiolite Complex is part of the Zagros Suture Zone (ZSZ) and is located within the Penjween-Walash Subzone northeast of Iraq. It is an incomplete sequence that consists of two main igneous bodies: the ultramafic body and the gabbroic body. The Penjween layered metagabbros show wide variation in grain size and are composed of saussuritized plagioclase, and amphibole with relict pyroxene. The chondrite-normalized REE patterns in Penjween metagabbroic rocks exhibit LREE depletion and flat MREE and HREE patterns, with patterns that are nearly flat in general, and these patterns are similar to rocks generated in Island Arc Tholeiite (IAT) and subduction-related environments. The depletion in High Field Strength Elements (HFSEs) with enrichment in Large Ion Lithophile Elements (LILEs) and the strong negative Nb anomaly is typical of magmas formed in the supra subduction zone. The La/Nb and La/Ba ratios indicate that metagabbroic rocks originated in the asthenosphere mantle, while the La/Yb and Dy/Yb ratios imply shallow source partial melting of spinel-peridotite. The variable Sr/Nd and Ba/Th ratios with nearly constant Th/Yb and La/Sm ratios, indicate that fluids from slab dehydration modified the ancient mantle. Penjween ophiolite metagabbros are classified as Island Arc Tholeiite (IAT) because it contains very low to low-TiO₂ (0.11-0.69%). In conclusion, the low and very low Ti concentration strongly suggests that the metgabbroic rocks of the Penjween Ophiolite Complex are linked to Island Arc Tholeiite, which has a link to the supra subduction zone.

© 2023 Jordan Journal of Earth and Environmental Sciences. All rights reserved

Keywords: Metagabbro, Ophiolite, Penjween, Geochemistry, Tectonic Setting, Iraq.

1. Introduction

Peridotites in the ophiolite complex generally involve serpentized harzburgites, lherzolite, dunite, and existing pyroxenite (Snow and Dick, 1995). These peridotites represent the bottom category of the ophiolite; these comprise sub-continental or orogenic Alpine ultramafic rocks (Menzies and Dupuy, 1991) and slivers of ancient oceanic lithosphere obducted onto the continental or oceanic crust (Beccaluva et al., 1984; Nicolas and Boudier, 2003). Moreover, the oceanic origin represents mantle rocks that were extracted along normal and transform faults (Bonatti et al., 1981). Igneous oceanic crust is a second part of this complex formed at divergent plate boundaries and consists of gabbro rocks, pillow lava, and diabasic dykes (Klein, 2004; Jassim and Goff, 2006). Ophiolite complexes' classification normally depends on their geochemical features, interior structures, and regional tectonics (Pearce et al., 1984; Shervais, 2001; Pearce, 2008). A new classification of ophiolite complexes proposed by Dilek and Furnes (2011) implies subduction-related ophiolite complexes which involve volcanic arc and supra subduction zone, and subduction-unrelated ophiolite complexes which involve mid-oceanic ridge (MOR), plume (P-type), and continental margin (CM).

Zagros Suture Zone encompasses the Penjween-Walash Subzone that consists of volcano-sedimentary sequences created in the Cretaceous ocean spreading of the Neo-Tethys and is strongly affected by magmatism (Buday and Jassim,

1987). During Paleocene-Eocene, the final closure of Neo-Tethys, Paleocene arc volcanic and syn-tectonic essential intrusions created (Aswad, 1999), thus the area represents the residues of the Neo-Tethys which during Miocene-Pliocene thrust over the Arabian Plate, such as Pleistocene Al-Lajjoun Basaltic flows, central Jordan (El-Hasan and Al-Malabeh, 2008), and Precambrian Magmatic Rocks (Al-Malabeh et al., 2004) besides elsic dike swarms in Aqaba complex (Al-Fugha et al., 2013). The Penjween-Walash Subzone is divided into three thrust sheets, the upper Qandil, the middle Walash, and the lower Napurdan (Jassim and Goff, 2006; Aswad et al., 2011; Mohammad et al., 2014; Ali et al., 2016). This subzone forms an almost unbroken swath over the Iraqi-Iranian borders. Qandil thrust sheet includes basic igneous massifs consisting of Hasanbag, Pushtashan, Bulfat, Mawat, and Penjween (Ali et al., 2019), the study area is located within this thrust sheet. Penjween igneous complex is located to the south-west of Penjween town, about 50 kilometers to the east of Sulaimani city between latitudes (35° 36' 16.4"- 35° 37' 15.6" N) and longitudes (45° 54' 40.4"- 45° 55' 54" E), (Figure 1).

Gabbros are part of the crustal portion in an ophiolite complex and consist of (from bottom to top) layered gabbros, isotropic and then foliated gabbros formed by slow crystallized basaltic melt injection from the fundamental rising mantle (Kakar et al., 2013). According to Al-Hassan and Hubbard (1985); Al-Hassan (1987), the gabbroic rocks of

* Corresponding author e-mail: omarsaif@uomosul.edu.iq

the Penjween ophiolite formed as a result of partial melting of the upper mantle, leaving depleted dunite rocks. In Albian-Cenomanian, the gabbros of Penjween were intruded on during the ocean spreading process (Jassim and Goff, 2006). In this study, we discuss the petrogenesis and tectonic environment of the Penjween ophiolite meta gabbroic rocks based on their field observations, petrography, and chemical compositions.

2. General Geology

The Penjween Ophiolite Complex is situated to the southwest of Penjween town about 50 kilometers east of Sulaimani City northeast of Iraq (Figure 1a). The area is part of the Zagros Suture Zone (ZSZ) and the complex is located within Penjween-Walash Subzone (Jassim and Goff, 2006). The ZSZ is subdivided into two allochthonous thrust sheets; lower and upper allochthonous (Aswad, 1999). The Penjween-Walash Subzone (i.e. upper allochthonous) represents the ophiolitic complexes and Albian-Cenomanian Gemo-Qandil sequence (Aswad and Elias, 1988; Aziz, 2008; Aswad et al., 2011; Aziz et al., 2011). The Walash-Naopurdan sequence (Paleocene-Eocene) represents the lower allochthon which is separated from the upper allochthon by a thrust fault (Aswad, 1999).

The Penjween Ophiolite Complex is an elongated body that covers about 35 km² inside the Iraqi territories towards northwest-southeast parallel with the general tectonic trend of the ZSZ, while the large remnant parts of this complex are located within and adjacent to Iranian territories (Mahmood, 1978). The sequence of Penjween ophiolite is incomplete (Jassim and Goff, 2006). It consists of ultramafic rocks mainly peridotite with subordinate pyroxenites followed by gabbros and minor occurrences of diorites, granodiorites, and pegmatites (Mahmood, 1978), that is in contact with a volcano-sedimentary sequence (i.e. Gimo Group) (Jassim and Goff, 2006). The group is thrust over Merga Red Beds (Miocene molasse) in the west. The ultramafic body form about 70% of the complex and consists of relatively fresh dunite (Jassim and Al-Hassan, 1977). The gabbro body represents the second largest exposure in the area (18 km² in extent in Iraq) sharply overlies the ultrabasic body and is layered and laminated (Jassim and Al-Hassan, 1977).

3. Materials and Methods

Twenty-one samples from the meta gabbroic rocks were collected from two different locations within the Penjween Ophiolite Complex. The current study employed a variety of analytical techniques, starting with the use of a polarized microscope for petrographic study and ending with chemical analysis. Five samples among the least weathered were selected to represent the freshest rocks prepared for chemical analysis. Before that the samples were ground in a swing mill and then the Loss on Ignition (LOI) was determined in the laboratories of the University of Mosul, Department of Geology. The geochemistry of whole rocks (major, trace, and rare earth elements) was analyzed in the ACME Analytical Laboratories, Canada, Vancouver done by 6000 ELAN ICP-MS. To prepare the samples for analysis, 0.25 mg of rock powder is digested using a multi-acid digestion (H₂O₂-HF-HClO₄-HNO₃), then heated on a hot plate, cooled, and finally

dissolved in 5% hydrochloric acid. The standards used in the analysis are OREAS 24P and OREAS 45P (For more information on analytical accuracy and precision, see Tables 1 and 2.). Since this ICP-MS analysis measures iron as FeO_t as it does not distinguish between ferric and ferrous oxides, it had to be measured and separated by ECIL CE 3021 Spectrophotometer at the Department of Geology, University of Mosul using the method of (Jeffery and Hutchison, 1981).

4. Results

4.1 Petrology and Petrography

Gabbro forms the second largest exposure in the area. It consists of a solid body extending to about 3 km of the upper and western edge of the mountain chain and southwest of Penjween village. These gabbros become a narrow sector in the northwest direction (Figure 1b). Gabbros are bordered by peridotite bodies as perpendicular and sharp contact and they are linked with the sandstones and conglomerates of the Merga Red Bed Group by a thrust fault near Kani Mangah village while they are in contact with Qandil metamorphic rock group in the southeastern direction. Depending on field observations and a previous study by Al-Hassan (1982) three types of gabbroic rocks are recognized in Penjween ophiolite; marginal gabbro, layered gabbro, and gabbro pegmatite (Figure 1b). Most gabbros in the field had suffered deformation in the form of fracturing and jointing (Figure 2b).

The metagabbros consist of saussuritized plagioclase, amphibole with relict pyroxene, chlorite, and opaque minerals. Some gabbros have been deformed, showing granular and porphyroclastic textures (Figure 2c, d). Also, these rocks show a schistosity texture (Figure 2e), those occurring along shear zones and western contact zone are severely crushed and foliated so much so that they impart schistosity to the rocks (Mahmood, 1978). The schistosity texture of Penjween metagabbros represents the thrusting movement and emplacement (Al-Hassan, 1982). Metagabbro also exhibits an ophitic and subophitic texture, with large crystals of amphibole completely or partially surrounding plagioclase (Figure 2f). The composition of plagioclase is An₇₀₋₇₃ refers to the labradorite. Plagioclase shows wide variation in grain size due to granulation (Figure 2d). In sheared and schistose rocks, Williams et al. (1954) believed that many of the feldspars are granulated. The deformed plagioclase are characterized by fractured surface, wavy extinction, bent lamellae and well developed secondary twin (Figure 2e). The saussurization process has partially changed the plagioclase grains into epidote (Figure 3a). A primary amphiboles have subhedral to anhedral grains, pleochroism that is primarily green to brown, and a cross-basal section that reveals two sets of cleavage (Figure 3b). Some amphibole grains have partially or completely altered to chlorite (Figure 3c). Primary amphibole shows kink bands due to deformation process along the shear zones (Figure 3d). The pyroxenes are mainly augite (extinction angle 42°). The minerals and textures are typical of metagabbros, which can form during low grade metamorphism from gabbros (Koyi et al., 2010; Hassan and Ridha, 2018).

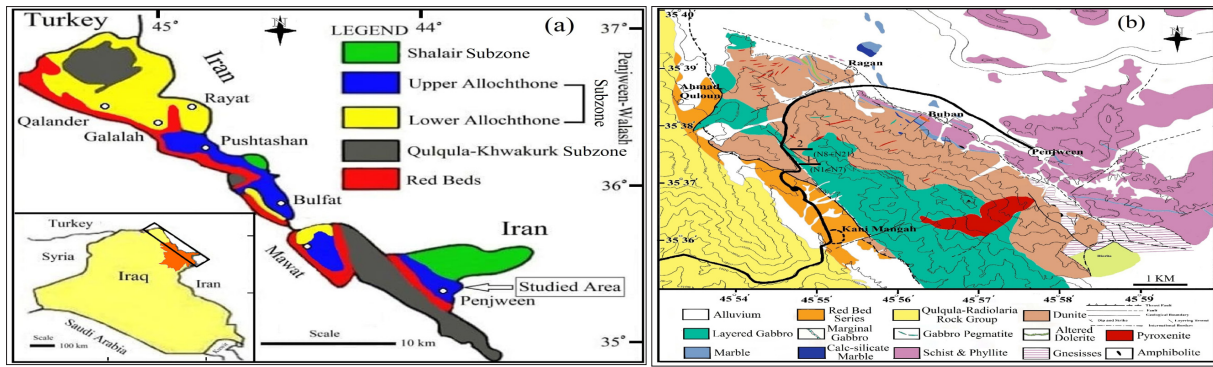


Figure 1. (a) Simplified geological map of the Zagros Suture Zone (ZSZ) showing the position of the study area; (b) Geological-topographic map of Penjween Ophiolite Complex, northeast Iraq, from (Al-Hassan, 1982) showing samples locations.

Table 1. Major and trace element composition for the Penjween ophiolite metagabbroic rocks, as well as accuracy, precision, and detection limits.

Elements	Sample No.					Analytical accuracy and precision					
	N31	N15	N14	N13	N12	R.N31	*45P	**45P	*24P	**24P	MDL
SiO ₂	51.06	50.44	48.35	46.64	45.59	-	-	-	-	-	-
TiO ₂	0.25	0.12	0.11	0.64	0.69	0.25	1.73	1.61	1.83	1.65	0.002
Al ₂ O ₃	10.73	13.03	16.66	14.73	15.79	10.26	12.88	12.90	14.47	14.70	0.04
FeO	7.77	5.97	4.89	8.64	8.64	8.06	24.72	23.43	9.68	9.39	0.03
Fe ₂ O ₃	0.32	0.75	1.20	4.13	5.24						
MnO	0.17	0.16	0.14	0.18	0.19	0.16	0.17	0.17	0.14	0.14	0.0003
MgO	13.53	13.31	11.99	9.42	8.03	13.23	0.32	0.32	6.85	6.73	0.03
CaO	12.24	12.86	13.81	12.61	12.63	12.13	0.42	0.42	8.16	8.09	0.03
Na ₂ O	1.38	0.52	0.52	0.49	0.69	1.35	0.11	0.11	3.15	3.36	0.003
K ₂ O	0.33	0.02	0.05	0.02	0.02	0.33	0.42	0.43	0.84	0.87	0.02
P ₂ O ₅	0.02	0.002	0.002	0.002	0.002	0.02	0.11	0.10	0.31	0.32	0.002
LOI	2.20	2.80	2.30	2.50	2.50	-	-	-	-	-	-
Total	100.01	100.01	99.99	100.01	99.99	-	-	-	-	-	-
#Mg*	74.93	78.11	78.16	57.59	51.69	-	-	-	-	-	-
Ni	246.9	142.5	136.7	178.7	54.7	245	385	380.30	141.0	144.1	0.10
Cr	563	325	254	61.0	14.0	571	1089	1061	196	182	1.00
Sc	48.0	53.2	43.8	67.2	64.6	48.20	67.10	64.90	20.00	19.20	0.10
V	266	195	157	1229	1203	266.00	267.00	263.00	158.00	156.00	1.00
Ba	101	2.00	2.00	20.0	6.00	101.00	296.00	289.00	285.00	266.00	1.00
Rb	3.40	0.20	0.70	0.40	0.60	3.70	24.60	23.00	22.40	20.90	0.10
Sr	89.0	40.0	54.0	53.0	68.0	88.00	32.60	34.00	403.00	382.00	1.00
Cs	0.30	0.10>	0.10>	0.10>	0.10>	0.28	2.00	2.20	0.80	0.80	0.10
Zr	5.80	1.00	0.70	1.20	3.00	6.10	154.00	154.30	141.00	138.40	0.20
Y	7.40	2.50	2.50	3.70	3.10	7.30	13.00	12.90	21.30	20.50	0.10
Nb	0.44	0.06	0.07	0.06	0.09	0.43	21.60	20.27	21.00	19.47	0.04
Ga	8.65	8.03	9.68	13.61	14.67	8.53	22.50	22.05	19.43	19.39	0.02
Cu	14.41	57.42	85.03	854.5	349	14.13	749.00	703.30	52.00	48.69	0.02
Zn	53.0	38.3	43.7	75.4	71.5	51.70	141.00	140.50	119.00	116.40	0.20
Pb	1.03	0.69	2.52	1.17	0.92	0.95	22.00	23.14	2.90	2.80	0.02
Mo	0.46	0.09	0.18	0.12	0.13	0.45	2.10	2.04	1.50	1.47	0.05
Co	67.2	56.6	51.6	81.4	72.5	66.20	120.00	121.70	44.00	48.10	0.20
As	0.70	0.70	0.20>	0.60	0.90	0.50	12.00	12.80	1.20	2.00	0.20
Cd	0.07	0.08	0.07	0.09	0.15	0.05	0.20	0.21	0.15	0.16	0.02
Sb	0.18	0.05	0.07	0.03	0.05	0.20	0.82	0.81	0.09	0.09	0.02
W	95.6	34.8	41.0	39.7	53.9	95.30	1.10	1.00	0.50	0.40	0.10
Li	8.70	1.60	1.30	1.10	1.40	8.50	14.70	15.90	8.70	8.40	0.10
Hf	0.25	0.05	0.04	0.06	0.11	0.30	4.12	3.76	3.60	3.33	0.02
Th	0.10	0.09	0.09	0.09	0.09	0.10	9.80	10.00	2.85	2.80	0.10
Ta	0.30	0.10>	0.10>	0.10>	0.10	0.23	1.20	1.30	1.04	1.10	0.10

* Mg# = 100 x Mg / (Mg + Fe²⁺).

R. N31 : Repeated N31.

45P** : Calculated OREAS45P, 45P* : Published OREAS45P.

24P** : Calculated OREAS24P, 24P* : Published OREAS24P.

MDL: Method Detection Limit.

Table 2. REE elements composition (in ppm) of the Penjween ophiolite metagabbroic rocks, as well as accuracy, precision, and detection limits.

REEs	Sample No.					Analytical accuracy and precision					
	N31	N15	N14	N13	N12	R. N31	45P*	45P**	24P*	24P**	MDL
La	0.50	0.20	0.10	0.30	0.20	0.60	24.80	25.10	17.40	17.90	0.10
Ce	1.30	0.16	0.14	0.56	0.26	1.36	48.90	51.26	37.60	38.25	0.02
Pr	0.20	<0.10	<0.10	0.20	<0.10	0.14	6.00	5.80	4.70	4.80	0.10
Nd	1.10	0.20	0.20	0.60	0.30	1.20	23.2	23.20	22.00	21.00	0.10
Sm	0.40	0.10	0.10	0.20	0.10	0.40	4.24	4.00	4.70	4.60	0.10
Eu	0.20	<0.10	<0.10	0.10	0.10	0.20	1.10	1.10	1.60	1.50	0.10
Gd	0.80	0.30	0.30	0.50	0.30	0.90	3.80	3.40	5.30	5.30	0.10
Tb	0.20	<0.10	<0.10	0.10	<0.10	0.20	0.59	0.50	0.81	0.70	0.10
Dy	1.20	0.50	0.50	0.70	0.60	1.20	3.60	3.60	4.60	4.60	0.10
Ho	0.30	0.10	<0.10	0.10	0.10	0.26	0.65	0.60	0.80	0.80	0.10
Er	1.00	0.40	0.30	0.50	0.40	1.00	1.70	1.70	2.20	2.20	0.10
Tm	0.10	<0.10	<0.10	<0.10	<0.10	0.10	0.24	0.20	0.30	0.30	0.10
Yb	1.00	0.40	0.40	0.50	0.40	0.90	1.60	1.50	1.83	1.70	0.10
Lu	0.20	<0.10	<0.10	<0.10	<0.10	0.20	0.24	0.30	0.25	0.20	0.10
Ratios											
Samples	N31	N15	N14	N13	N12	Samples	N31	N15	N14	N13	N12
(La/Yb) _N	0.36	0.36	0.18	0.43	0.36	Dy/Yb	1.20	1.25	1.25	1.40	1.50
(Gd/Yb) _N	0.66	0.62	0.62	0.83	0.62	Sr/Nd	80.91	200	270	88.33	226.7
La/Nb	0.45	1.00	0.50	0.50	0.67	Ba/Th	1010	22.2	22.2	222.2	66.67
La/Ba	0.005	0.10	0.05	0.02	0.03	Th/Yb	0.10	0.23	0.23	0.18	0.23
La/Yb	0.50	0.50	0.25	0.60	0.50	La/Sm	1.25	2.00	1.00	1.50	2.00

R. N31 : Repeated N31.

45P** : Calculated OREAS45P, 45P* : Published OREAS45P.

24P** : Calculated OREAS24P, 24P* : Published OREAS24P.

MDL: Method Detection Limit

4.2 Major Oxides

The MgO-CaO-Al₂O₃ diagram (Colleman, 1977) has been used to differentiate between ultramafic and mafic cumulate rocks. Based on that the metagabbroic rocks of Penjween ophiolite are classified as mafic cumulate rocks (Figure 4a). The TAS diagram (Cox et al., 1979) shows that the Penjween ophiolite metagabbroic rocks are sub alkaline character (Figure 4b). On the AFM diagram, the Penjween ophiolite metagabbros exhibit the nature of tholeiitic igneous rocks (Figure 4c). The Penjween metagabbro rocks are classified largely as low-K rocks (Figure 4d). Generally, the

Penjween metagabbros have a low content of TiO₂ (0.11 to 0.69 wt %), and P₂O₅ (0.002 to 0.02 wt %), K₂O (0.02 to 0.33 wt %) and Na₂O (0.49 to 1.38 wt %), with modest variations in SiO₂ (45.59 to 51.06 wt %), while the Al₂O₃, FeO, Fe₂O₃, MgO, and CaO have wide ranges and high concentrations, these ranges are 10.73 to 16.66 wt %, 4.89 to 8.64 wt %, 0.32 to 5.24 wt %, 8.03 to 13.53 wt %, and 12.24 to 13.81 wt % respectively (Table 1). Moreover, the metagabbros have very low total alkali concentrations, where Na₂O+K₂O values are between 0.51 to 1.7 wt% with the K₂O value much lower than Na₂O.

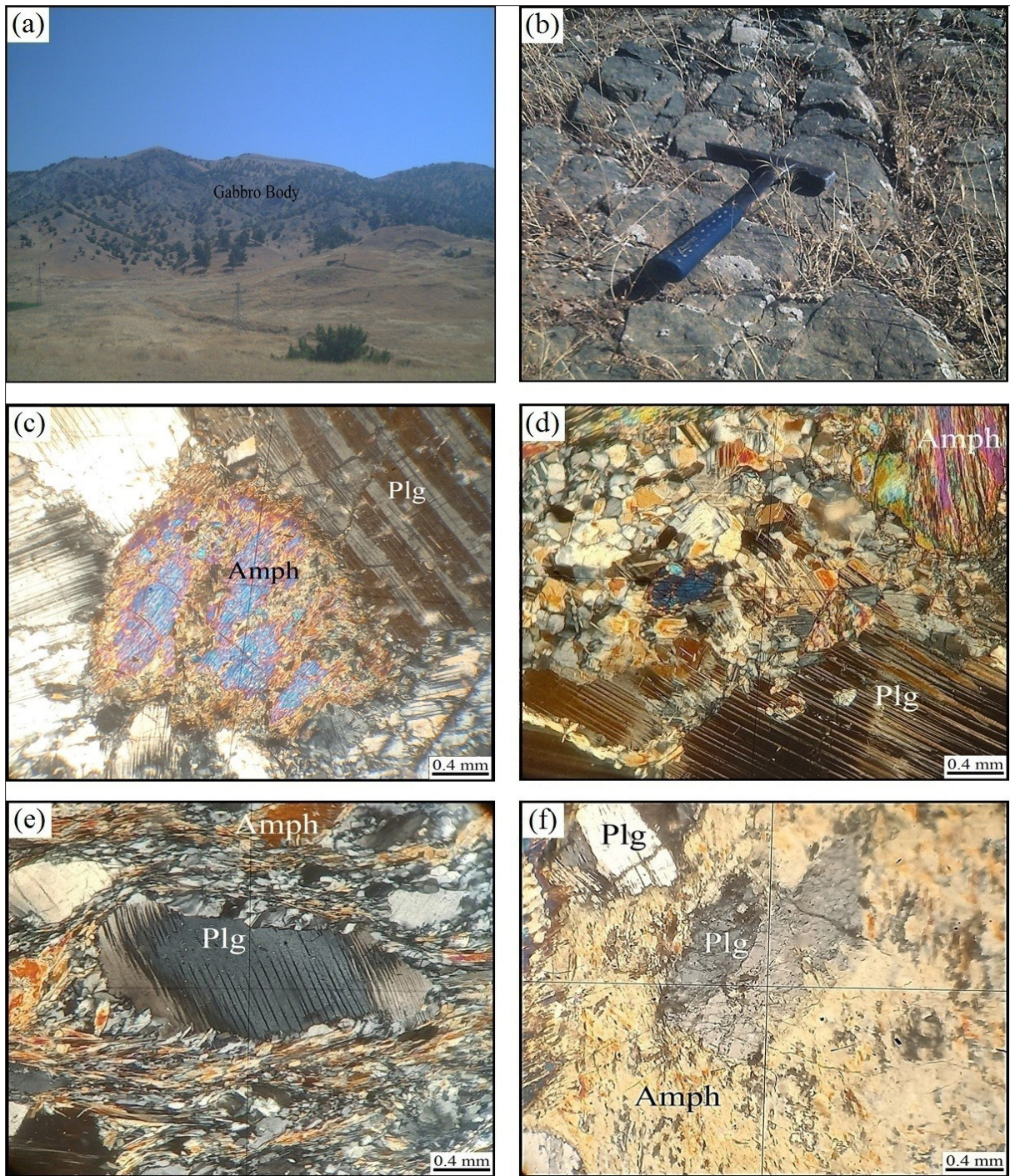


Figure 2. Field photos and photomicrographs showing: (a) Panoramic view of the studied gabbro; (b) Metagabbro fracturing and jointing, sample N11; (c) Granular textures in metagabbro, sample N10; (d) Porphyroclastic texture in metagabbro and the plagioclase show wide variation in grain size due to granulation, sample N14; (e) Metagabbro show schistosity texture and secondary twin lamellae in plagioclase, sample N12; (f) Ophitic and subophitic texture, sample N10; [Plg: Plagioclase; Amph: Amphibole; Opq: Opaque].

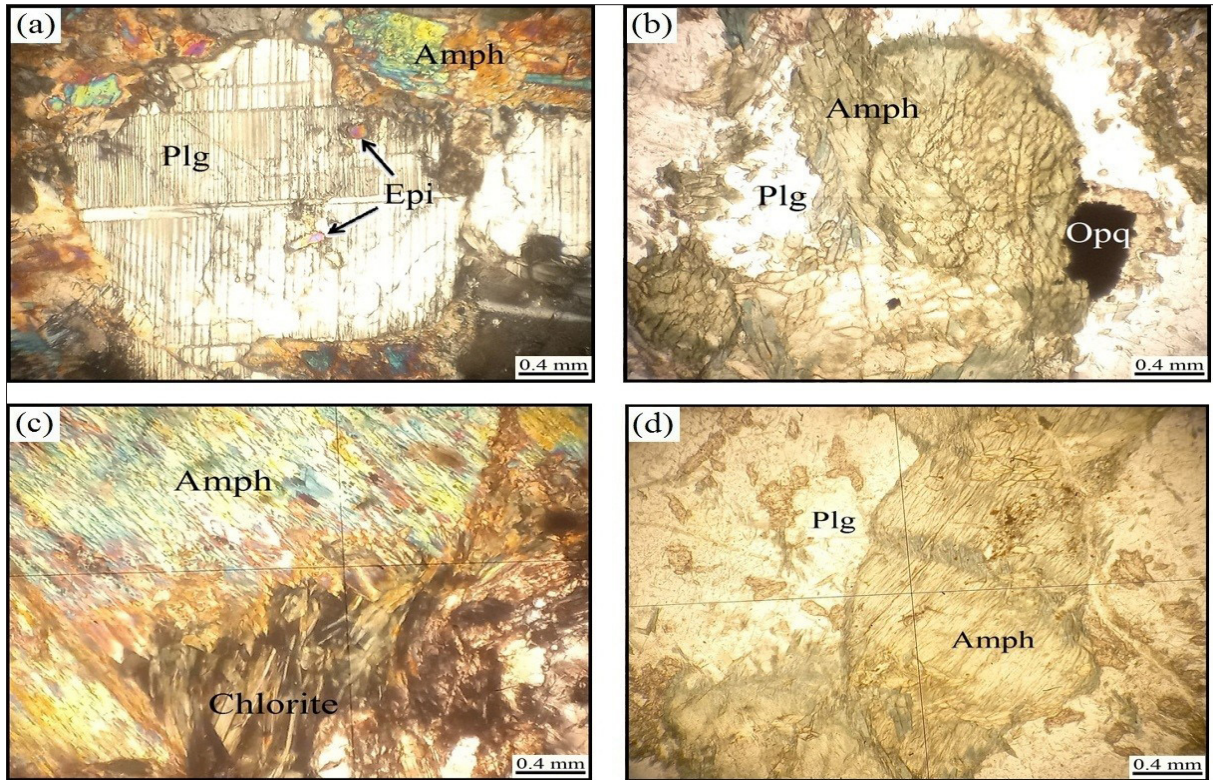


Figure 3. Photomicrographs showing: (a) Saussuritization process has partially changed the plagioclase grains into epidote, sample N5; (b) Amphibole has two sets of cleavage (56/124°), sample N6; (c) Alteration of amphibole into chlorite, sample N4; (d) Amphibole with kink bands, sample N4, [Plg: Plagioclase; Amph: Amphibole; Epi: Epidote; Opq: Opaque].

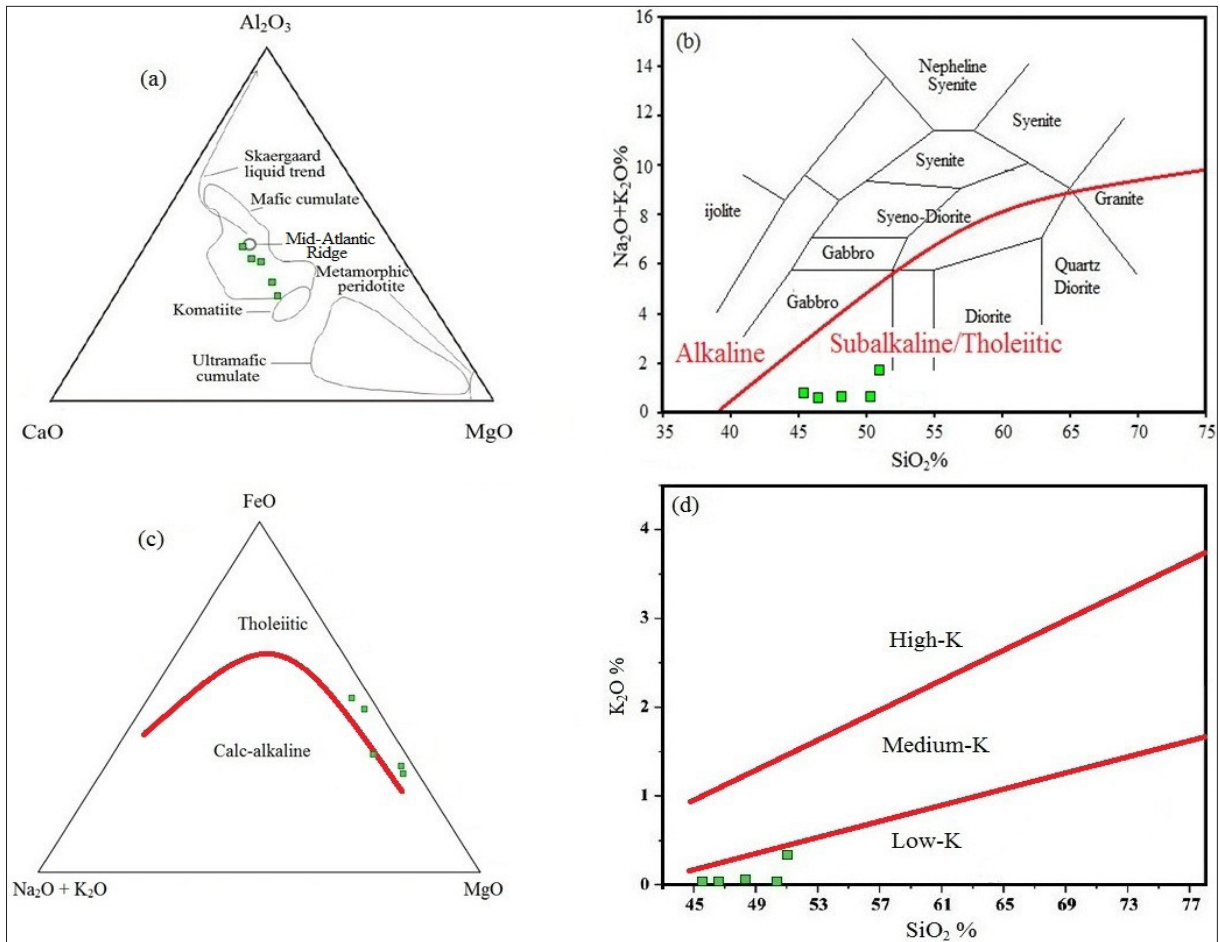


Figure 4. Geochemical classifications of the Penjween metagabbroic rocks: (a) CaO-Al₂O₃-MgO diagram for the Penjween ophiolite metagabbroic rocks (Coleman, 1977); (b) TAS plot of the gabbros (Cox et al., 1979); (c) AFM diagram (Irvin and Baragar, 1971) of metagabbros from Penjween Ophiolite Complex indicating their tholeiitic affinity; (d) SiO₂ vs. K₂O diagram (Le Maitre, 2002).

4.3 Trace and Rare Earth Elements (REEs)

Both Large Ion Lithophile Elements (LILE) and the High Field Strength Elements (HFSE) have variable amounts in the Penjween metagabbros, like Ba (2-101 ppm), Sr (40-89 ppm), Rb (0.2-3.4 ppm), Pb (0.69-2.52 ppm), Zr (0.7-5.8 ppm), Nb (0.06-0.4 ppm), and Y (2.5-7.4 ppm) (Table 1). LIL elements (Ba, Rb, Sr, and K) are thus probable to have been remobilized during alteration and metamorphism to greenschist facies (Staudigel, 2003).

The REEs in the Penjween metagabbro rocks are generally characterized by relatively parallel REE patterns with enrichment of HREE and depletion in light rare earth elements (LREE) [(La/Yb)_N = 0.36-0.43]. These ratios indicate the enrichment of these rocks in HREE and MREE compared to LREE (Figure 5a). The spider diagram (multi elements) exhibits depletion in HFSEs like Zr, Nb, Y, and Hf with enrichment in LILEs like Sr, Ba, Rb, and Pb (Figure 5b). The depletion in Nb and LREE refers to a source originating from the lower crust (Taylor and McLennan, 1985), it is characteristic of magmas formed in the supra-subduction mantle wedge (Duclaux et al., 2006). Pearce et al. (1984) assumed that the eclectic enrichment of Ba and Sr in comparison to Zr, and Y shown by tholeiitic rocks is typical of a supra-subduction zone (SSZ) setting where tholeiitic and boninitic magma mixing happens.

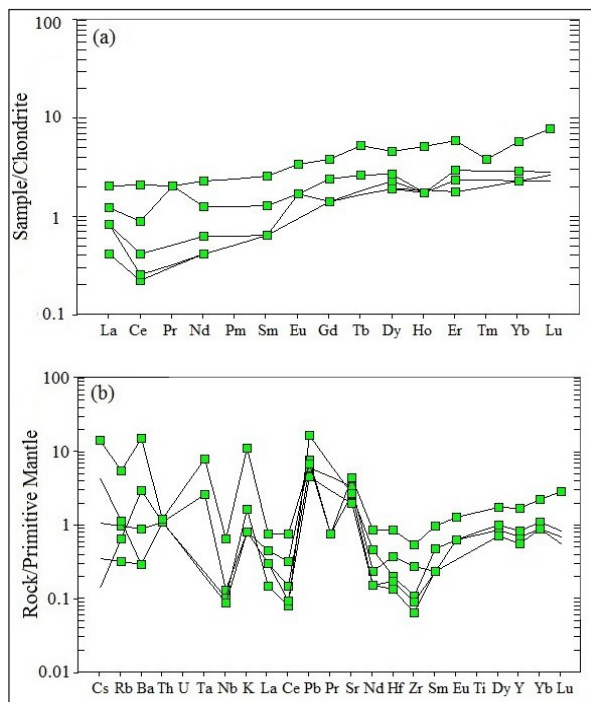


Figure 5. (a) Chondrite-normalized REE patterns of metagabbroic rocks from Penjween ophiolite (Sun and McDonough, 1989); (b) Primitive mantle-normalized spider diagram of metagabbroic rocks of Penjween ophiolite (Sun and McDonough, 1989).

5. Discussion

5.1 Petrogenesis

Magmatic rocks derived from primary magma typically have a high Mg number ($Mg\# > 65$) (Winter, 2001; Al Smadi et al., 2018). The samples from the Penjween metagabbro have a high $Mg\#$ (68.1), indicating that the metagabbros are the result of primary magma crystallization. REEs and HFSEs are immobile during the weathering and alteration processes (Zhang et al., 2015). As a result, magma origins are determined largely using the ratios and contents of HFSEs and LREEs (Zhao and Zhou, 2007). Most metagabbros fall in the asthenosphere mantle origin in the La/Nb-La/Ba diagram (Figure 6a). The La/Yb ratios have a range of 0.25-0.6, and the Dy/Yb ratios of the metagabbroic rocks are concentrated in a limited range of 1.2-1.5, reflecting shallow source partial melting of spinel-peridotite (Figure 6b) (Thirlwall et al., 1994). Penjween metagabbro mantle metasomatism was also revealed by the La/Sm against Ba/Th diagram (Labanieh et al., 2012) and the Th/Yb against Sr/Nd diagram (Woodhead et al., 1998). As seen in figures (6c, d) the Penjween metagabbros deviate from the sediment melting trend while being consistent with slab dehydration, suggesting that fluids from slab dehydration modified the mantle. The depletion in HFSEs like Zr, Nb, Hf, and Pb refers to the separating of LILE such as Sr, Ba, Rb, and HFSEs during subducting slab dehydration (Shawna et al., 2003). Moreover, the depletion of HFS elements may result from fractionation and metamorphism processes (John et al., 2004). In summary, the Penjween metagabbro formed as a result of partial melting of the mantle spinel peridotite that has been metasomatized by fluids dehydrated from a subducted slab (Wang et al., 2019).

The relation between Y and Cr (Figure 7a) proves that the amount of Cr varies with a nearly constant in Y; which is a characteristic of a mantle source depleted (Shinjo et al., 2000). The relationship between Ni and Cr is significant in determining ferromagnesian mineral fractionation (Leeman, 1976). Figure (7b) shows that clinopyroxene is the main ferromagnesian phase existing in Penjween metagabbros, based on the positive trend between Ni-Cr and the absence of olivine in all samples. This indicates that it was derived from a previous fractionated origin or a melt that was extensively fractionated mostly by removing olivine (Wilson, 2001). On Ti against Ti/Cr and Ti against Al_2O_3/TiO_2 (Figure 7c, d), the crystallization trends of the main phases parallel the trends of plagioclase and clinopyroxene. As a result, these minerals are the major crystalline phases, as Al-Hassan (1982) demonstrated in the Penjween gabbroic rocks.

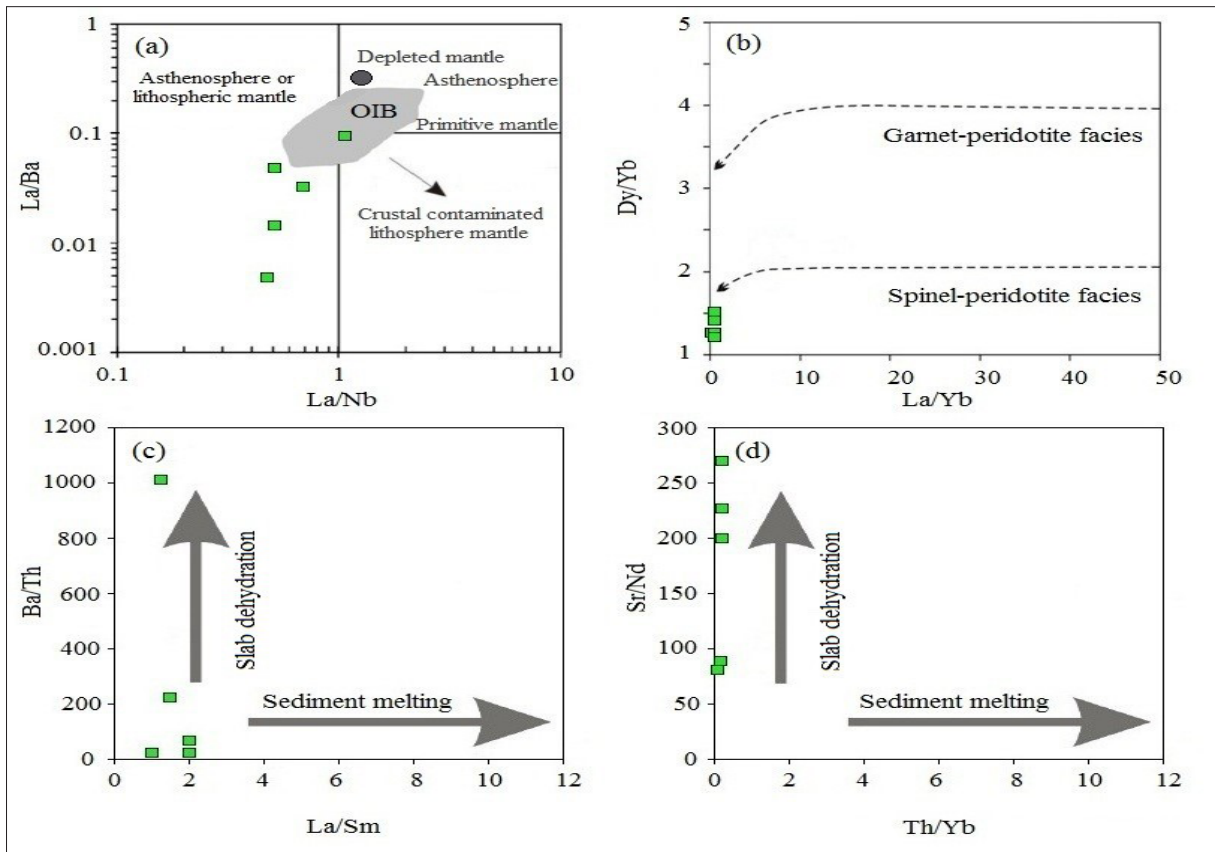


Figure 6. (a) La/Ba vs. La/Nb diagram (Saunders et al., 1992); (b) La/Yb vs. Dy/Yb diagram (Jung et al., 2006); (c) La/Sm vs. Ba/Th for the Penjween metagabbros (Labanich et al., 2012); (d) Th/Yb vs. Sr/Nd for the Penjween metagabbros (Woodhead et al., 1998).

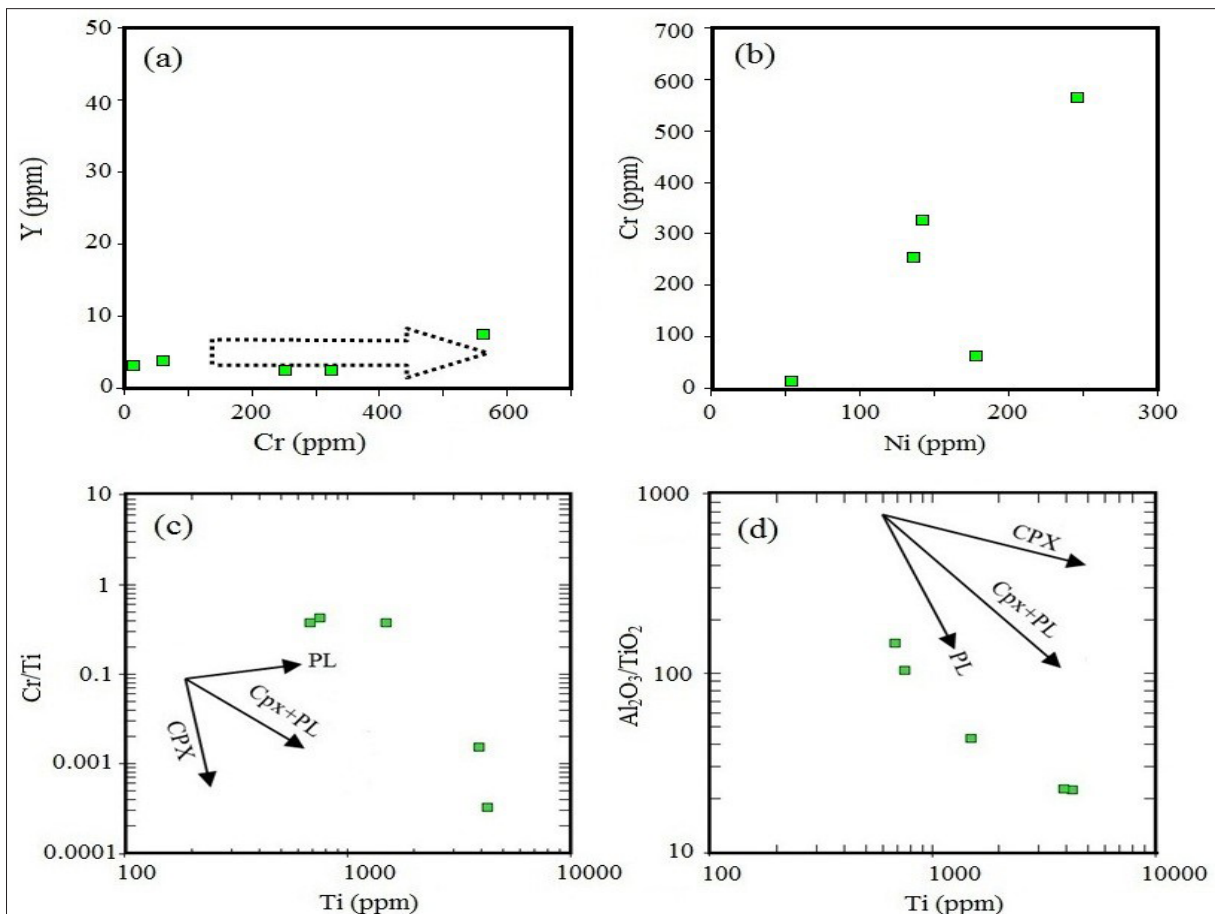


Figure 7. (a) Cr vs. Y diagram shows a depleted mantle source (Shinjo et al., 2000); (b) Ni vs. Cr; (c) Ti vs. Cr/Ti diagram (Pearce and Flower, 1977); (d) Ti vs. Al₂O₃/TiO₂ diagram (Pearce and Flower, 1977).

5.2 Tectonic Setting

In general, all studied metagabbros of the Penjween ophiolite are geochemically related and have a tholeiitic character. Zr-Nb-Th diagram classifies these metagabbros as Island Arc Tholeiite (IAT) (Figure 8a). Therefore, maybe these metagabbroic rocks have been created in the extensional environment (low pressure) by fractional crystallization directly in the supra-subduction zone or above a subduction zone (Kakar et al., 2013). The AFM diagram shows the Penjween metagabbro rocks occur into the arc-related mafic cumulate rock (Figure 8b), this is confirmed that these rocks are created from fractionation of the primary magma via depleted mantle in the magma chamber (Sarifakioglu et al., 2009). All these indicate that Penjween ophiolite metagabbroic rocks are created in a supra-subduction zone environment (Beard, 1986).

The IAT nature of the metagabbroic rocks from the Penjween ophiolite is further evidenced by their REE and spider diagrams (Figure 5a, b). Generally, the chondrite-normalized REE patterns in Penjween metagabbroic rocks exhibit LREE depletion and flat MREE and HREE patterns, with patterns that are nearly flat in general, and these patterns are similar to rocks generated in IAT and subduction-related environments (Shamim et al., 2005). The features exhibited on the spider diagram show enrichments of Sr and Ba and the relative depletion of Y, Zr, and Hf these patterns as well as HFSEs variances in the tholeiitic rocks represent the SSZ setting (Pearce et al., 1984). The depletion in HFSEs with enrichment in LILEs and the strong negative Nb anomaly (Figure 5b) are typical of a magma formed in the supra-subduction zone (Whattam et al., 2004).

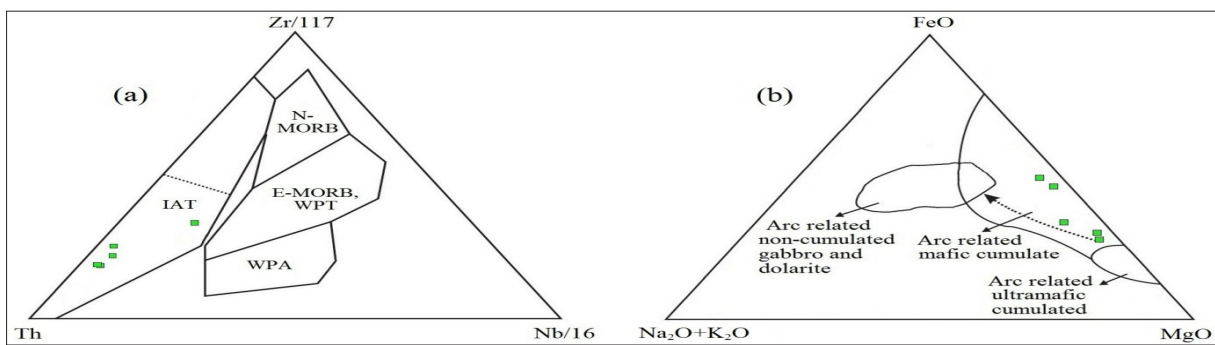


Figure 8. Tectonomagmatic diagrams of the Penjween ophiolite metagabbroic rocks: (a) Zr-Nb-Th diagram (Wood, 1980); (b) AFM compositions of metagabbros in Penjween ophiolite. The non-cumulate and cumulate rocks are from Beard (1986).

The Al_2O_3 - TiO_2 diagram shows these metagabbros are located in the arc-related magma setting (Figure 9a), whereas all metagabbroic rocks show that the magma is related to subduction on the Zr-Th-Nb diagram (Figure 7a). Figures (9b, c) show that metagabbroic rocks are generally low-Ti and very low-Ti Island Arc Tholeiitic (IAT), indicating that they are generated in a subduction zone. Penjween ophiolite metagabbros contain very low to low- TiO_2 (0.11-

0.69%) concentrations and were probably derived from IAT magmas, which are formed in supra-subduction zone environments (Beccaluva et al., 1989). In conclusion, the low and very low Ti concentration strongly suggests that the metagabbroic rocks of the Penjween Ophiolite Complex are linked to Island Arc Tholeiite, which has a link to the supra subduction zone, as Mirza (2008) demonstrated in the Mawat gabbros.

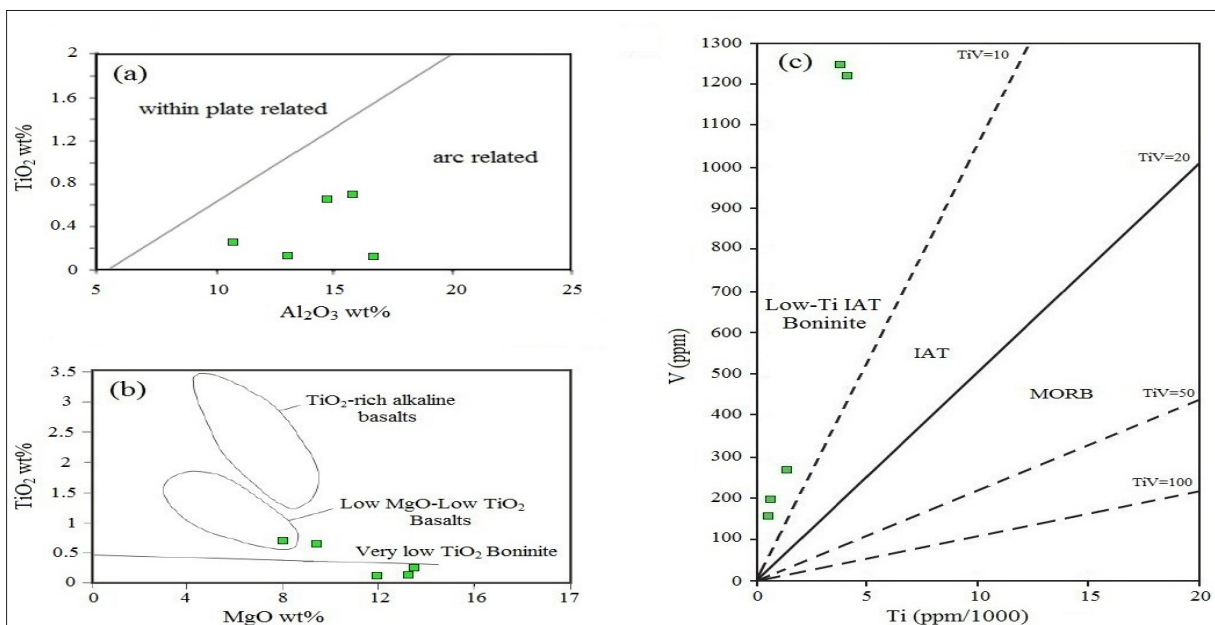


Figure 9. Tectonomagmatic diagrams of the Penjween ophiolite metagabbroic rocks: (a) Al_2O_3 vs. TiO_2 diagram (Muller and Groves, 1997); (b) MgO vs. TiO_2 diagram (Laurent and Hebert, 1989); (c) Ti vs. V petrogenetic discrimination diagram (Shervais, 1982)

6. Conclusion

Penjween ophiolite complex consists of ultramafic rocks followed by gabbros and minor occurrences of diorites, granodiorites, and pegmatites. The metagabbros are composed of saussuritized plagioclase, amphibole with relict pyroxene, chlorite, and opaque minerals. Some metagabbros have been deformed, showing granular and porphyroclastic textures, also these rocks show a schistosity texture. The mineral and textures are typical of metagabbros, which can form from gabbros under low-grade conditions. The geochemical indicators exhibit a substantial variance in major elements content, modest variations in SiO_2 , low contents of TiO_2 , and P_2O_5 , with high contents and wide ranges of MgO , FeO , Fe_2O_3 , Al_2O_3 , and CaO . Penjween metagabbro rocks have tholeiitic igneous characteristics and are mostly low-K rocks with very low total alkali concentrations. Penjween metagabbro has a high Mg\# , indicating that it formed from primary magma crystallization. Geochemical characteristics of the Penjween ophiolite metagabbros demonstrate that these rocks were generated by partial melting of the mantle spinel peridotite that has been metasomatized by fluids dehydrated from a subducted slab. The IAT nature and supra-subduction zone environments of the Penjween ophiolite metagabbroic rocks are confirmed by their REE and HFSEs patterns. The tectonic environment diagrams confirm that the metagabbroic rocks have island arc-related, and also that the TiO_2 concentrations in the Penjween ophiolite metagabbros are very low to low. As concluded, the low and very low Ti content suggests that the Penjween Ophiolite Complex metagabbroic rocks are linked to Island Arc Tholeiite, which is linked to the supra subduction zone.

Acknowledgments

The authors are very grateful to the College of Sciences, University of Mosul for providing facilities, which help to improve the quality of this work. So, we would like to thank Dr. Azzam H. Al-Samman for his helpful and constructive review, which improved the manuscript. The authors are very grateful to the Editor in Chief, the Secretary of the Journal, and the Technical Editors for their great efforts and valuable comments.

References

- Al Smadi, A., Al-Malabeh, A., Odat, S. (2018). Characterization and Origin of Selected Basaltic Outcrops in Harrat Irbid (HI), Northern Jordan. *Jordan Journal of Earth and Environmental Sciences* 9(3): 185-196.
- Al-Fugha, H., El-Hasan, T., Al-Malabeh, A., Hamaideh, A., El-Mezayen, A. (2013). Mineralogy, Geochemistry, and Origin of Felsic Dike Swarms in Aqaba Complex (Wadi Al-Yutum), South Jordan. *Arabian Journal of Geosciences* 6(10): 3979-3987.
- Al-Hassan, M.E. (1982). Petrology, Mineralogy, and Geochemistry of Penjwin Igneous Complex, Northeast Iraq, Ph.D. Thesis, University of Dundee.
- Al-Hassan, M.E. (1987). Rare-Earth Element Pattern of Layered Gabbro, Penjwin Complex, NE Iraq, In *Geochemistry of Ophiolites*, edited by Delaloye, M. and Bechon, F., Ofioliti, pp. 437-444.
- Al-Hassan, M.E., and Hubbard, F.H. (1985). Magma Segregations in a Tectonic Remnant of Basalt Ophiolite, Penjween, NE Iraq. In: *Ophiolites through Time*; Proceedings, edited by Desmons, J., Ofioliti. pp. 139-146.
- Ali, S.A., Ismail, S.A., Nutman, A.P., Bennett, V.C., Jones, B.G., Buckman, S. (2016). The Intra-Oceanic Cretaceous (~108 Ma) Kata-Rash Arc Fragment in the Kurdistan Segment of Iraqi Zagros Suture Zone: Implications for Neotethyan Evolution and Closure. *Lithos* 260: 154-163.
- Ali, S.A., Nutman, A.P., Aswad, K.J., Jones, B.G. (2019). Overview of the Tectonic Evolution of the Iraqi Zagros Thrust Zone: Sixty Million Years of Neotethyan Ocean Subduction. *Journal of Geodynamics* 129: 162-177.
- Al-Malabeh, A., Al-Fugha, H., El-Hasan, T. (2004). Petrology and Geochemistry of Late Precambrian Magmatic Rocks from Southern Jordan. *Neues Jahrbuch für Geologie und Paläontologie* 233(3): 333-350.
- Aswad, K.J. (1999). Arc-Continental Collision in Northeastern Iraq as Evidence by the Mawat and Penjween Ophiolite Complex. *Rafidain Journal of Science* 10: 51-61.
- Aswad, K.J. and Elias, E.M. (1988). Petrogenesis, Geochemistry, and Metamorphism of Spilitized Subvolcanic Rocks of the Mawat Ophiolite Complex, NE Iraq. *Ofioliti* 13: 95-109.
- Aswad, K.J., Aziz, N.R., Koyi, H.A. (2011). Cr-spinel Compositions in Serpentinites and their Implications for the Petrotectonic History of the Zagros Suture Zone, Kurdistan Region, Iraq. *Geological Magazine* 148(5-6): 802-818.
- Aziz, N.R., 2008. Petrogenesis, Evolution, and Tectonics of the Serpentinites of the Zagros Suture Zone, Kurdistan Region, NE Iraq. Ph.D. Thesis, University of Sulaimani.
- Aziz, N.R., Aswad, K.J., Koyi, H.A. (2011). Contrasting Settings of Serpentine Bodies in the Northwestern Zagros Suture Zone, Kurdistan Region, Iraq. *Geological Magazine* 148: (5-6), 819-837.
- Beard, J.S. (1986). Characteristic Mineralogy of Arc Related Cumulate Gabbros: Implications for the Tectonic Setting of Gabbroic Plutons and Andesite Genesis. *Geology* 14: 848-851.
- Beccaluva, L., Macciotta, G., Piccardo, G.B., Zeda, O. (1989). Clinopyroxene Composition of Ophiolite Basalts as Petrogenetic Indicator. *Chemical Geology* 77: 165-182.
- Beccaluva, L., Macciotta, G., Piccardo, G.B., Zeda, O., 1984. Petrology of Lherzolithic Rocks from the Northern Apennine Ophiolites. *Lithos*, 17, 299-316.
- Bonatti, E., Hamlyn, P.R., Ottonello, G. (1981). The Upper Mantle Beneath a Young Oceanic Rift: Peridotites from the Island of Zabargad (Red Sea). *Geology* 9: 474-491.
- Buday, T. and Jassim, S.Z. (1987). The Regional Geology of Iraq: Tectonism, Magmatism, and Metamorphism, edited by Kassab, I.M. and Abass, M.J., Geological Survey, and Mineral Investigation, Baghdad.
- Colleman, R.G. (1977). *Ophiolites: Ancient Oceanic Lithosphere*. Springer-Verlag, New York.
- Cox, K.G., Bell, J.D., Pankhurst, R.J. (1979). *The Interpretation of Igneous Rocks*. George Allen & Unwin, London.
- Dilek, Y. and Furnes, H. (2011). Ophiolite Genesis and Global Tectonics: Geochemical and Tectonic Fingerprinting of Ancient Oceanic Lithosphere. *Geological Society of America Bulletin* 123: 387-411.
- Duclaux, G., Menot, R.P., Guillot, S., Agbossoumonde, Y., Hilaret, N. (2006). The Mafic Layered Complex of the Kabye' Massif (North Togo and North Benin): Evidence of a Pan-African Granulitic Continental Arc Root. *Journal of Precambrian Research* 151: 101-118.
- El-Hasan, T. and Al-Malabeh, A. (2008). Geochemistry, Mineralogy and Petrogenesis of El-Lajjoun Pleistocene Alkali Basalt of Central Jordan. *Jordan Journal of Earth and Environmental Sciences* 1(2): 53-62.
- Hassan, D.K. and Ridha, A.H. (2018). Petrography and Mineralogy of Amphibolite Rocks in Penjween Complex, Northeastern Iraq. *International Journal of Advanced Engineering*

- Research and Science. 5(2): 146-157.
- Irvine T.N. and Baragar W.R. (1971). A Guide to Chemical Classification of the Common Volcanic Rocks. Canadian Journal of Earth Sciences, 8, 523-548.
- Jassim, S.Z. and Al-Hassan, M.I. (1977). Petrography and Origin of the Mawat and Penjwin Igneous Complexes: A Comparison. Journal of Geological Society of Iraq Special Issue: 169-210.
- Jassim, S.Z. and Goff, J.C. (2006). Geology of Iraq. Dolin, Prague and Moravian Museum, Brno.
- Jeffery, P.G. and Hutchison, D. (1981). Chemical Methods of Rock Analysis. Pergamon Series in Analytical Chemistry. Pergamon Press, Oxford.
- John, T., Scherer, E.E., Haase, K., Schenk, V. (2004). Trace Elements Fractionation During Fluid. Included Eclogitization in a Subducting Slab: Trace Element and Lu-Hf-Sm-Nd Isotope Systematics. Journal of Earth and Planetary Science Letters 227: 441-456.
- Jung, C., Jung, S., Hoffer, E., Berndt, J. (2006). Petrogenesis of Tertiary Mafic Alkaline Magmas in the Hoheifel, Germany. Journal of Petrology 47: 1637-1671.
- Kakar, M.I., Mahmood, K., Khan, M., Kasi, A.K., Abdul Manan, R. (2013). Petrology and Geochemistry of Gabbros from the Muslim Bagh Ophiolite: Implications for their Petrogenesis and Tectonic Setting. Journal of Himalayan Earth Sciences, 46(1): 19-30.
- Klein, E.M. (2004). Geochemistry of the Igneous Oceanic Crust, In Treatise on Geochemistry, edited by Holland, H.D. and Turekian, K.K., Elsevier Pergamon, Oxford, pp. 433-464.
- Koyi, A.M.A., Sofyissa, M.M., Jameel, N.M. (2010). Geochemistry of Metagabbros from Southern Mawat Ophiolite Complex, NE Iraq. Journal of Pure and Applied Sciences. 22(4): 30-46.
- Labanieh, S., Chauvel, C., Germa, A., Quidelleur, X. (2012). Martinique: A Clear Case for Sediment Melting and Slabdehydration as a Function of Distance to the Trench. Journal of Petrology 53: 2441-2464.
- Laurent, R. and Heberi, R. (1989). The Volcanic and Intrusive Rocks of the Quebec Appalachian Ophiolites (Canada) and their Island Arc Setting. Chemical Geology 77: 287-302.
- Le Maitre, R.W. (2002). Igneous Rocks: A Classification and Glossary of Terms. Cambridge University Press, Cambridge, and New York.
- Leeman, W.P. (1976). Petrogenesis of Mckinney (Snake River) Olivine Tholeiite in the Light of Rare-Earth Elements and Cr/Ni Distributions. Geological Society of America Bulletin 87: 1582-1586.
- Mahmood, L.A. (1978). Petrology of the Ultramafics Around Penjwin, Northeast of Iraq with Special References to the Genesis of the Chromites Associated with them, M.Sc. Thesis, University of Mosul.
- Menzies, M.A. and Dupuy, C. (1991). Orogenic Massifs: Protolith, Process, and Provenance. Orogenic Lherzolite and Mantle Processes. Journal Petrology Special: 1-16.
- Mirza, T.A. (2008). Petrogenesis of the Mawat Ophiolite Complex and Associated Chromitite, Kurdistan region, NE Iraq. Ph. D. Thesis, University of Sulaimani.
- Mohammad, Y.O., Cornell, D.H., Qaradaghi, J.H., Mohammad, F.O. (2014). Geochemistry and Ar-Ar Muscovite Ages of the Daraban Leucogranite, Mawat Ophiolite, Northeastern Iraq: Implications for Arabia-Eurasia Continental Collision. Journal Asian Earth Science 86:151-165.
- Muller, D. and Groves, D. (1997). Potassic Igneous Rocks and Associated Gold-Copper Mineralization. Springer-Verlag, Berlin, Heidelberg.
- Nicolas, A. and Boudier, F. (2003). Where Ophiolite Come From and What Do They Tell us? Geological Society of America, Boulder, USA, Special Paper 373: 137-152.
- Pearce, J.A. (2008). Geochemical Fingerprinting of Oceanic Basalts with Applications to Ophiolite Classification and the Search for Archean Oceanic Crust. Lithos 100: 14-48.
- Pearce, J.A. and Flower, M.F.J. (1977). The Relative Importance of Petrogenetic Variables in Magma Genesis at Accreting Plate Margins: a Preliminary Investigation. Journal of the Geological Society, London 134: 103-127.
- Pearce, J.A., Lippard, S.J., Roberts, S. (1984). Characteristics and Tectonic Significance of Supra-Subduction Zone Ophiolites, In Marginal Basin Geology, edited by Kokelaar, B.P. and Howells, M.F., Geological Society, London. pp. 77-89.
- Sarifakioglu, E., Ozen, H., Winchester, J.A. (2009). Petrogenesis of the Refahiye Ophiolite and its Tectonic Significance for Neotethyan Ophiolites Along the Izmir-Ankara-Erzincan Suture Zone. Turkish Journal of Earth Sciences 18: 187-207.
- Saunders, A.D., Storey, M.; Kent, R.W., Norry, M.J. (1992). Consequences of Plume-Lithosphere Interactions, In Magmatism and the Causes of Continental Break-up, edited by Alabaster, T., Storey, B.C., Pankhurst, R.J., Geological Society, London, UK. pp. 41-60.
- Shamim, K.M., Smith, T.E., Raza, M., Huang, J. (2005). Geology, Geochemistry and Tectonic Significance of Mafic-Ultramafic Rocks of Mesoproterozoic Phulad Ophiolite Suite of South Delhi Fold Belt, NW Indian Shield. Journal of Gondwana Research, 8(4): 553-566.
- Shawna, M., Leatherdale, Maxeiner, R.O., Ansdell, K.M. (2003). Petrography and Geochemistry of Love Lake Lecogabbro, Swan River Complex, Peter Lake Domain, Northern Jour. Saskatchewan, Saskatchewan Geological Survey 2: 1-17.
- Shervais, J.W. (1982). Ti-V Plots and the Petrogenesis of Modern and Ophiolitic Lavas. Earth and Planetary Science Letters 59: 101-18.
- Shervais, J.W. (2001). Birth, Death, and Resurrection: the Life Cycle of Suprasubduction Zone Ophiolites. Geochemistry, Geophysics, Geosystems 2: 1010.
- Shinjo, R., Woodhead, J.D., Hergt, J.M. (2000). Geochemical Variation within the Northern Ryukyu Arc: Magma Source Compositions and Geodynamic Implications. Contributions to Mineralogy and Petrology 140: 263-282.
- Snow, J.E. and Dick, H.J.B. (1995). Pervasive Magnesium Loss by Marine Weathering of Peridotites. Geochim. Geochimica et Cosmochimica Acta 59: 4219-4235.
- Staudigel, H. (2003). Hydrothermal Alteration Processes in the Oceanic Crust, In Treatise on Geochemistry, edited by Holland, H.D., Turekian, K.K., Elsevier Pergamon. Oxford. pp. 511-535.
- Sun, S. and McDonough, W. (1989). Chemical and Isotopic Systematics of Oceanic Basalts: Implications for Mantle Composition and Processes, In Magmatism in the Ocean Basins, edited by Saunders, A.D., Norry, M.J., Geological Society London. pp. 313-345.
- Taylor, S.R. and McLennan, S.M. (1985). The Continental Crust: Its Composition and Evolution. Blackwell, Oxford.
- Thirlwall, M.F., Upton, B.G.J., Jenkins, C. (1994). Interaction between Continental Lithosphere and the Iceland Plume: Sr-Nd-Pb Isotope Chemistry of Tertiary Basalts, NE Greenland. Journal of Petrology 35: 839-897.
- Wang, J.P., Wang, X., Liu, J.J., Liu, Z.J., Zhai, D.G., Wang, Y.H. (2019). Geology, Geochemistry, and Geochronology of Gabbro from the Haoyaoerhudong Gold Deposit, Northern Margin of the North China Craton. Minerals 9(63): 1-18.
- Whattam, S., Malpas, J., Ali, J., Smith, I.E.M., Hualo, C. (2004). Origin of the Northland Ophiolite, Northern New Zealand: Discussion of New Data and Reassessment of the Model. Journal of Geology and Geophysics 47: 383-389.
- Williams, H., Turner, F.J., Gillbert, C.M. (1954). Petrography:

- An Introduction to the Study of Rocks in Thin Sections. Freeman and Company, San Francisco.
- Wilson, S.A. (2001). The Geochemical Analysis of Siluro-Devonian Mafic Dikes in the 15' Woodsville Quadrangle, East-Central Vermont, Senior Thesis, Middlebury College, Middlebury, Vermont.
- Winter, J. (2001). Introduction to Igneous and Metamorphic Petrology; Prentice Hall: Upper Saddle River, New Jersey, USA.
- Wood, D.A. (1980). The Application of a Th-Hf-Ta Diagram to Problems of Tectono-Magmatic Classification and to Establishing the Nature of Crustal Contamination of Basaltic Lavas of the British Tertiary Volcanic Province. *Earth and Planetary Science Letters*, 50(1): 11-30.
- Woodhead, J.D., Eggins, S.M., Johnson, R.W. (1998). Magma Genesis in the New Britain Island Arc: Further Insights into Melting and Mass Transfer Processes. *Journal of Petrology* 39: 1641-1668.
- Zhang, B.L., Lv, G.X., Su, J., Shen, X.L., Liu, R.L., Liu, J.G., Hai, L.F., Zhang, G.L. (2015). A Study of the Tectono-Lithofacies Mineralization Regularities of the Gejiu tin Polymetallic Orefield, Yunnan, and Prospecting in its Western Part. *Earth Science Frontiers* 22: 078-087.
- Zhao, J.H. and Zhou, M.F. (2007). Geochemistry of Neoproterozoic Mafic Intrusions in the Panzihua District (Sichuan Province, SWChina): Implications for Subduction-Related Metasomatism in the Upper Mantle. *Precambrian Research* 152: 27-47.